

The Correlation Between Surface Chemistry, Surface Morphology, and Cycling Efficiency of Lithium Electrodes in a Few Polar Aprotic Systems

Doron Aurbach* and Yosef Gofer

Chemistry Department, Bar-Ilan University, Ramat Gan 52100, Israel

Jacob Langzam

Life Science Department, Bar-Ilan University Ramat Gan 52100, Israel

ABSTRACT

Lithium electrodes in a few selected polar aprotic electrolyte systems were investigated using electrochemical techniques in conjunction with surface-sensitive Fourier transform infrared spectroscopy and scanning electron microscopy. The solvents used were γ -butyrolactone (BL), propylene carbonate (PC), and tetrahydrofuran (THF), and the salts included LiClO_4 and LiAsF_6 . Cycling efficiency of lithium electrodes was correlated to their surface chemistry and morphology in the various solvent systems. The effects of both water and oxygen contamination were rigorously studied. It was found that the presence of oxygen in solutions considerably increased the cycling efficiency of the lithium electrode. This effect correlates well with the influence of the presence of oxygen on the surface morphology of lithium electrodes in solutions. The presence of water increases cycling efficiency of Li electrodes in PC, and decreases cycling efficiency of Li electrodes in ethers. These results are discussed in light of the surface chemistry of lithium electrodes in the various solvent systems.

One of the challenges in modern electrochemistry is to improve the cycling efficiency of lithium electrodes in polar aprotic electrolyte systems comprised of organic solvents and Li salts, where lithium is apparently stable. The achievement of high reversibility for lithium electrodes will obviously advance the development of reliable commercial secondary batteries of the highest energy density. A variety of polar aprotic solvent systems have been investigated in the past two decades (1, 2). Several attempts to correlate lithium cycling efficiency with the physical and electrical properties of the polar aprotic media (e.g., conductivity, solvation parameters, viscosity, etc.) have been reported (3, 4).

However, it is widely believed that the major factor that controls the electrochemical behavior of the lithium electrode in polar aprotic systems is the nature of the films formed on the electrode surface (5, 6). Several research groups have tried to improve the reversibility of lithium electrodes in polar aprotic systems by modifying the 'natural' surface films by an addition of traces of active reagents to the solutions (7-10). Consequently, we have investigated in recent studies the nature of surface films formed on lithium electrodes in four important polar aprotic solvents: γ -butyrolactone (BL) (11), propylene carbonate (12), THF, and dimethoxy ethane (DME) (13). Surface-sensitive Fourier transform infrared (FTIR) (11-13), and to some extent also x-ray photoelectron spectroscopy (XPS) (12-13) and SIMS (13) techniques were applied. We also investigated the electrochemical behavior of these four solvent systems with noble metal electrodes (14-16).

This work (14-16) has the advantage that electro-reduction of the solvents and contaminants, which occur simultaneously on lithium surfaces, could be explored separately on noble metal electrodes at low potentials, since these processes are very potential-dependent (the reduction potential of oxygen dissolved in polar aprotic solvents, for instance, is about 2V more positive than that of lithium deposition) (17-18). In all four solvent-noble metal systems, the presence of oxygen and water was found to affect lithium dissolution and deposition processes (15, 16).

The present work aims to study the effect of water and trace O_2 on the reversibility of lithium electrodes in BL, PC, and THF, and to correlate cycling efficiency of Li electrodes in these systems to surface morphology, studied by scanning electron microscopy (SEM), and surface chemistry, studied by FTIR. It was interesting to explore

whether O_2 or H_2O contaminants may be used as surface modification agents for Li electrodes in these solvents, since these contaminants pronouncedly affect Li deposition on noble metals in these solvents (14-16). The influence of the salt anion on surface morphology and cycling efficiency of the Li electrode was also studied and is discussed in light of elemental analysis data obtained from Li electrodes treated in these electrolyte systems.

Experimental

The electrochemical measurements and all the preparations for the spectral studies were carried out at room temperature under a high purity argon atmosphere in Vacuum Atmospheres Corporation (VAC, USA) glove boxes fitted with HE 493 dry trains (VAC) for moisture and oxygen removal. Oxygen and moisture levels in the glove boxes were monitored continuously by a 1431-DP Ondyne (USA) moisture analyzer and a 317AX Teledyne (USA) oxygen analyzer, and were usually in the ppm level. Water concentration in the solutions was measured with a Metrohm (Swiss) 652 Karl Fisher Coulometer.

Materials.—High purity γ -butyrolactone (Merck), propylene carbonate (Aldrich), tetrahydrofuran (Frutarom, Israel), $\text{LiClO}_4 \cdot 3\text{H}_2\text{O}$ (Alfa product), LiAsF_6 (USS Agricultural), lithium foils 1 mm thick (Foote Minerals), and high purity argon, oxygen and nitrogen (Oxygen Center, Israel) were used. Purification of solvents and salts as well as the preparation of oxygen- or water-contaminated solutions has been described elsewhere (11-13, 19).

Instrumentation.—The electrochemical treatments and measurements were carried out with a PAR potentiostat (Model 173) fitted with a digital coulometer (Model 179), programmer (Model 175) and Yokogawa XY recorder (Model 3083). FTIR spectra were obtained with a Nicolet 60SXB spectrometer equipped with a di triglycine sulfate (DTGS) detector. The sample chamber of the spectrometer provides isolation from the room atmosphere and was constantly purged with dry air or nitrogen (CO_2 -free, dew point of -60°F). Solvent purity analysis by GCMS was carried out with a Finnigan 4000 mass spectrometer. In most cases a two-meter glass column filled with SP 1000 0.1% CarboPack C (Supelco) was used. NMR analysis was carried out with a Bruker AM 300 spectrometer. SEM measurements were carried out with JSM 840 scanning electron microscope (JEOL).

Electrochemical measurements.—Cycling efficiency measurements were carried out in the cell shown in Fig. 1.

*Electrochemical Society Active Member.

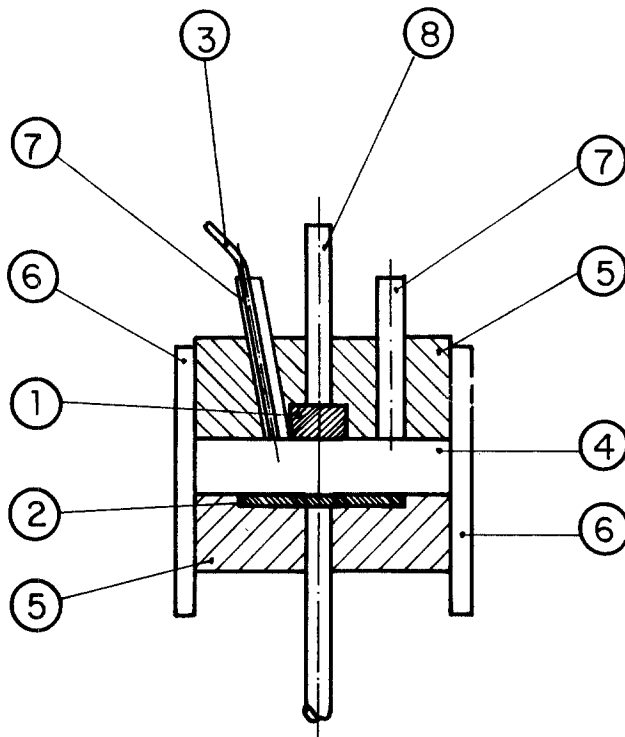


Fig. 1. The cell used for cycling efficiency measurements of lithium electrodes: 1) nickel or copper disk (working electrode) on which lithium is deposited; 2) lithium disk, counterelectrode attached to a copper rod; 3) lithium wire reference electrode; 4) a space for solution; 5) polyethylene bodies in which the electrodes are embedded; 6) a Teflon cylinder; and 7) glass tubes.

An initial amount of lithium (several coulombs per cm^2) was deposited on a nickel or copper electrode. Then, 10–30% of this initial amount was discharged (Li dissolution) and recharged (Li deposition) periodically, galvanostatically. In most cases the number of cycles was 5–15 and the current density was 0.5 mA/cm^2 or 1 mA/cm^2 , which is the same current density applied to lithium samples that were prepared for spectroscopic measurements. After cycling, the residual lithium was dissolved galvanostatically (same current density). We found that the initial deposition also has a limited efficiency which is quite similar to the average cycling efficiency. Therefore the average cycling efficiency could be calculated from the following equation

$$X = [q_c - (Xq_1 - q_r)/N]/q_c \quad [1]$$

where $100X$ is the cycling efficiency (%), N is the number of cycles, q_c , q_1 , and q_r are the charges involved in a single deposition process (half cycle), initial loading (massive lithium deposition), and final discharge (after cycling) respectively. The potential of the working electrode (*vs.* Li/Li^+ reference electrode) was continuously recorded during the whole experiment. The final dissolution process was interrupted when the working electrode potential exceeded 1V *vs.* Li/Li^+ .

Typical measurements of working electrode potential changes during cycling efficiency experiments are illustrated in Fig. 2. A periodic galvanostatic operation of the cell described in Fig. 1 was carried out by triggering the PAR (Model 173) potentiostat (set to galvanostatic mode) by a square waveform generator built specially for these experiments.

Spectroscopic measurements.—The FTIR measurements of Li electrodes are described in detail elsewhere (11–13). The SEM measurements were conducted as follows. After the electrochemical treatments, the electrodes were taken out of the cell, washed (pure solvent) and dried (evacuation). Pieces were cut from each electrode and were loaded on the transfer system built for this work.

Figure 3 shows the transfer system built for the SEM studies. The samples are loaded in the glove box on the

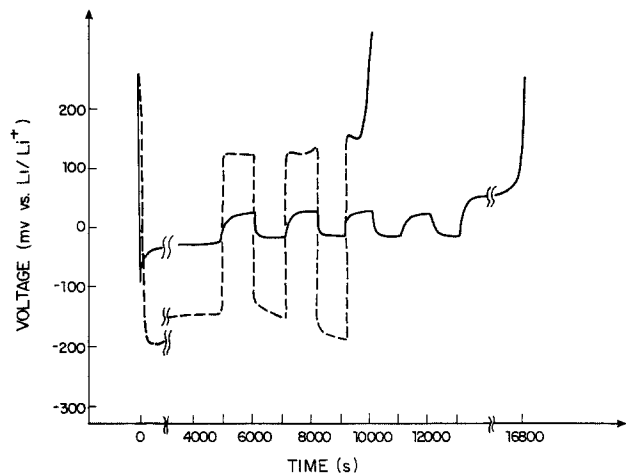


Fig. 2. Results of a typical experiment measuring cyclic efficiency of lithium electrode in the cell shown in Fig. 1. LiClO_4 $0.5\text{M}/\text{BL}$ solution. Galvanostatic charge-discharge cycling, 0.5 mA/cm^2 . The charge involved in initial lithium deposition was about 2.5 C/cm^2 . The last process was dissolution of the residual lithium. The dashed line indicates uncontaminated solution, and the solid line, oxygen-saturated solution.

sample tray [11] (see Fig. 3). Then, the sample tray [11] is introduced to the cylinder [2] by the manipulator [13], and put on tray [4] inside the cylinder [2]. Then the samples are isolated by pressing the disk [5] toward the 'O' ring [12] of the sample tray [11]. The whole system is taken out of the glove box. The cylinder [2] fits exactly to the port of the microscope [1]. It is pressed toward the 'O' ring [3]. The whole system is evacuated and reaches a pressure of about 10^{-5} torr. The disk [5] is lifted by screwing the bolts [10]. The sample tray [11] is moved with the manipulator [13] inside the microscope, where the pressure is about 10^{-6} torr. Using this method, the lithium samples are exposed only to the glove box atmosphere and to a vacuum of about 10^{-5} – 10^{-6} torr.

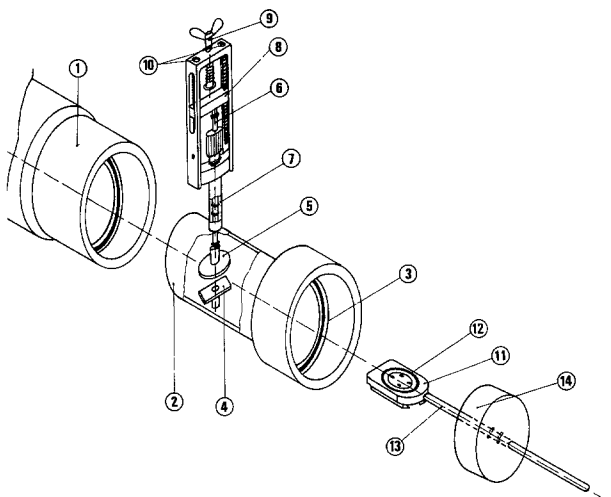


Fig. 3. The transfer system built for a transfer of lithium samples from the glove boxes to the scanning electron microscope: 1) electron microscope inlet; 2) the system's body (a brass cylinder); 3) rubber 'O' rings; 4) a fixed tray; 5) a brass disk (hermetically closes the samples in the sample tray [11] when being pressed toward 'O' ring [12]); 6) a brass shaft (presses or raises disk [5]); 7) a brass cylinder with two rubber 'O' rings which is welded to the body [2] and holds the shaft [6]; 8) a bridge attached to the edge of the shaft [6]; 9) a butterfly bolt by which the bridge [8] and the shaft [6] are pressed down; 10) two bolts with which the bridge [8], the shaft [6], and the disk [5] are raised upwards in order to release the sample tray when the system is evacuated, attached to the microscope; 11) the sample tray—The samples (pieces of lithium electrodes) are held in the middle attached to the tray by the four small belts; 12) a rubber 'O' ring; 13) manipulator (a stainless steel rod); 14) a Perpex cover in which the manipulator moves, held in two 'O' rings.

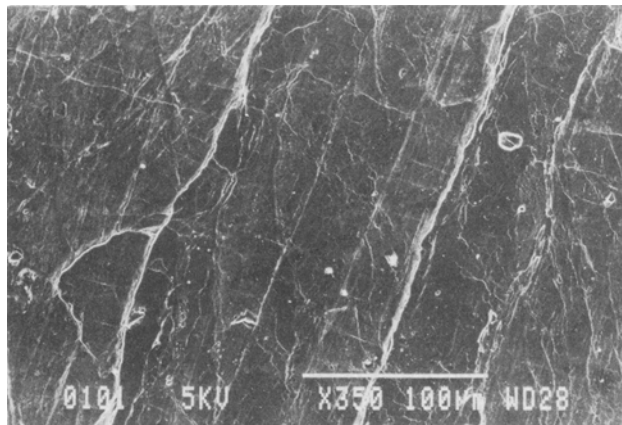


Fig. 4. Typical SEM micrograph of lithium surface before any electrochemical treatment. (Magnification = 350X. Scale appears in the micrograph.) The surface layer was sheared off followed by smoothing the surface with a glass tube.

Results and Discussion

Uncontaminated LiClO₄ solutions.—Figure 4 shows a typical SEM micrograph of a smooth, mirror-like lithium surface which was prepared by shearing off the surface layer (scraping it with a stainless steel knife), followed by smoothing (rolling it with a clean glass tube). Figure 5 shows SEM micrographs obtained from Li surfaces on which lithium was galvanostatically deposited from LiClO₄ solutions of THF, PC, and BL (5a, 5b, and 5c, respectively). Single dendrites at higher magnification are shown in Fig. 6a and 6b (obtained from PC and BL/LiClO₄ solutions, respectively). These micrographs show typical locations of dendrite formation (along cracks or stress lines). Also, the dendrites, as shown, have a lot of narrow regions (bottlenecks) where corrosion or mechanical shock can easily disconnect them from the bulk. We carried out a series of experiments in which Li electrodes were charged (Li deposition), followed by consecutive discharge (Li dissolution) in the various systems. The charge involved in the anodic process was in excess of 10% of the cathodic one. In all cases, the dissolution process leaves many dendrites untouched, and holes are formed. In other experiments, Li electrodes were cycled 5-30 times, followed by prolonged dissolution (twice the charge involved in a single half cycle) as a final process. SEM studies of these electrodes show that the density and average size of the dendrites left increase as a function of number of cycles. Table I summarizes the data obtained from the cycling efficiency measurements of Li electrodes in the various systems.

All the LiClO₄ salt solutions studied in this work have quite a poor lithium cycling efficiency. It should be noticed that the values of Table I are somewhat lower than cycling efficiency values of same solvents that appear in the literature (20-22). There are two major reasons for these differences:

1. The values of Table I were obtained from experiments in which lithium was deposited on nickel or copper substrates. Naturally, lithium deposition on a lithium substrate is expected to have a higher efficiency, since adherence of Li deposits to lithium substrate is better (23).

2. We found that in several solvent systems, cycling efficiency increases as electrolyte concentration increases (24). A maximum cycling efficiency of lithium electrode in PC-LiClO₄ was achieved at salt concentration around 1M (20).

In the present work, salt concentration in most of the experiments was around 0.5M, which is somewhat lower than the electrolyte concentrations where maxima in cycling efficiency of lithium electrodes are achieved (20, 21, 23). The poor lithium cycling efficiency obtained in the three solvent systems (which correlate nicely with the SEM studies indicating massive dendrite formation during Li deposition) should be discussed in light of the surface chemistry of lithium electrodes in these solvents ob-

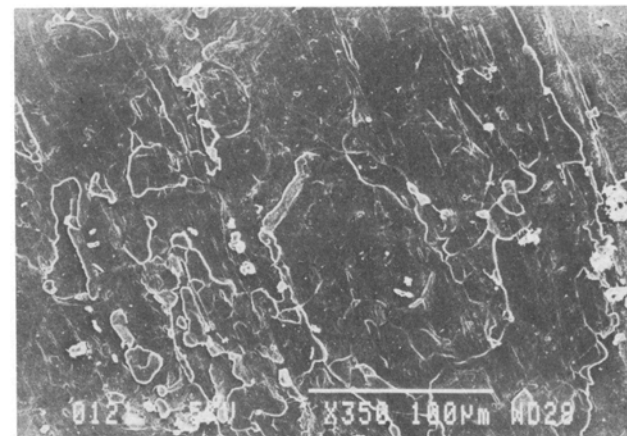
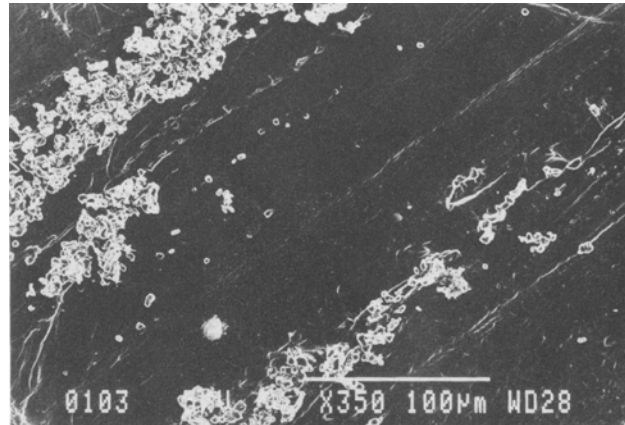


Fig. 5. Typical SEM micrographs obtained from lithium electrodes on which lithium was galvanostatically deposited (0.6-0.7 C/cm², 0.5 mA/cm²; 5a) LiClO₄ 0.5M/THF solution; 5b) LiClO₄ 0.5M/PC solution; 5c) LiClO₄ 0.5M/BL solution. Same magnification (350X) in (a)-(c). Scale appears in each micrograph.

tained by the FTIR measurements. It is generally accepted that the electrochemical behavior of lithium electrodes in polar aprotic solvents is surface films-controlled (5, 6). Since the resistance of these films to lithium cation transport is the main activation barrier to the electrochemical deposition or dissolution of lithium, the effectiveness and uniformity of Li cation passage through these films are the key factors which determine the cycling efficiency of lithium electrodes.

The transport of lithium cations through these films obviously depends on the different lithium-containing functional groups of the organic and inorganic molecules which build the films. These functional groups include alkyl carbonate (ROCO₂Li) and inorganic carbonate Li₂CO₃ in the case of PC (12), organic carboxylate (R-COOLi), alkoxy (R-O-Li), and β -keto ester anion in the case

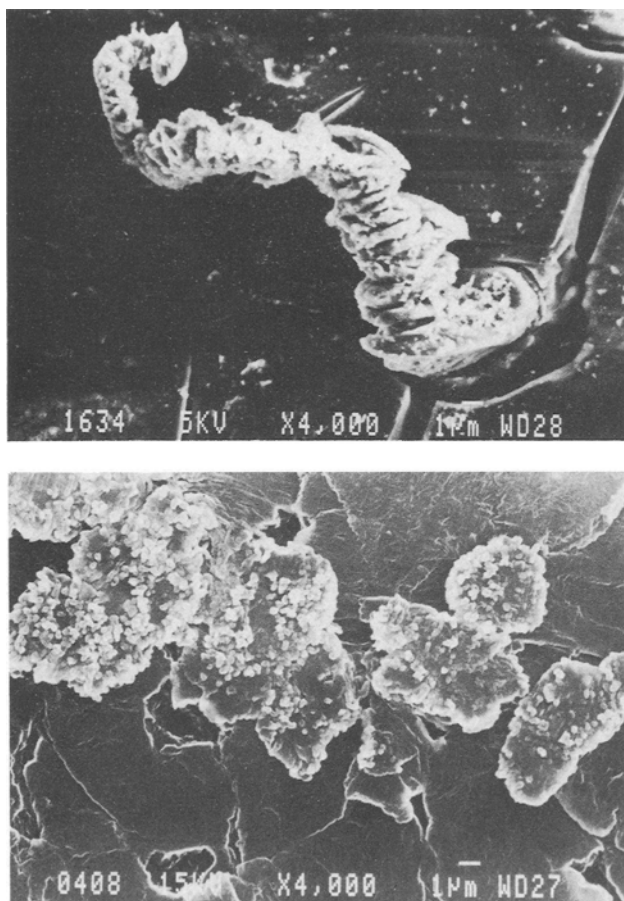


Fig. 6. Typical SEM micrographs of single dendrites formed by lithium deposition ($0.6\text{--}0.7 \text{ C}/\text{cm}^2$, $0.5 \text{ mA}/\text{cm}^2$): (a) LiClO_4 0.5M/PC solution (X4000); (b) LiClO_4 0.5M/BL solution (X4000).

of BL (11), and alkoxy groups in the case of the ethers (13). As was discussed elsewhere (11, 13), all of these surface species are formed by a complex mechanism involving electron transfer, bond cleavages, and radical termination stages. The nature of the 'R' groups (the alkyl part) in all of the above surface compounds is supposed to influence lithium transport through the films, since it may determine the orientation of the various compounds on the surface and, therefore, which of the functional groups will be dominant as lithium transfer agent. The radical termination stages are not completely understood. However, they may be influenced by local changes on the lithium surface. Hence, the initial morphology of surfaces may induce deposition of different surface species which differ from each other by their 'R' groups and therefore may also differ in orientation and participation in lithium cation transfer. The more different the types of surface species (and hence lithium-containing functional groups), the less uniform lithium transport through these films should be (which means dendritic Li deposition).

The ethers, which are far less reactive to lithium than BL or PC, are expected to form the most uniform films. However, this relative unreactivity of the solvents causes surface chemistry of lithium in ethers to be much more sensitive to the presence of contaminants in solutions. Hence, similar non-uniformity of lithium cation transfer, as found in cases of the more reactive PC or BL, also characterizes surface films formed on lithium in the less reactive ethers. Therefore, as pure systems, none of the LiClO_4 solutions studied seem to be adequate for secondary lithium batteries. Nevertheless, one should not give up on their use in rechargeable lithium systems, because other alternative solvent-electrolyte systems where much higher cycling efficiency of Li electrode has been obtained (22) (e.g., LiAsF_6 - 2 methyl THF) have disadvantages such as narrower electrochemical windows (24), volatility of solvents, medium conductivity, and toxicity of the electrolyte. Also, LiClO_4 is less poisonous than other salts such as LiAsF_6 . PC or BL have wide electrochemical windows (which enable the use of cathodes such as MnO_2 which have high redox potential), good conductivity, and low volatility and toxicity. Therefore, a study of modified electrolyte systems based on these solvents seems to have merit.

The influence of oxygen.—Table I shows that the presence of O_2 in solution considerably increases cycling efficiency and decreases polarization required for galvanostatic charge or discharge processes of Li electrodes in all the above solvent systems. These results seem to be in line with the surface morphology studies. Figure 7 shows two SEM micrographs obtained from lithium samples on which lithium was deposited in 0.3M LiClO_4 THF solutions. Micrograph 7a was obtained from a lithium electrode treated in oxygen-saturated solution, while micrograph 7b was obtained from a reference sample treated in uncontaminated solution.

Figure 8 shows a typical SEM micrograph obtained from a lithium electrode on which lithium was deposited in O_2 -saturated PC-0.5M LiClO_4 solution. (Its reference sample is shown in micrograph 5b.) The comparison of micrographs 7a and 8 to those of the reference samples clearly indicates that the presence of oxygen considerably suppresses dendrite formation in these systems during lithium deposition. Lithium electrodes were also cycled (consecutive deposition-dissolution processes) in oxygen-saturated THF and PC solutions. In both cases, SEM micrograph electrodes show that the lithium surfaces are left quite smooth, while those treated in uncontaminated THF or PC were densely covered with undissolved dendrites. These results mean that even if some dendrites are formed in oxygen-contaminated THF or PC solutions, they disappear more easily during consecutive dissolution processes than those formed in uncontaminated systems.

Lithium electrodes in oxygen-contaminated BL solutions behave differently. While lithium is deposited in uncontaminated BL solutions in flake-like dendrites (as shown in Fig. 5c and 6b), when oxygen is present in LiClO_4 /BL solutions, lithium is deposited in long, needle-like dendrites, as shown in Fig. 9a. Figure 9b shows a single dendrite at higher magnification. In spite of the many bottlenecks that each of these dendrites has (see Fig. 9b), all of the dendrites formed by deposition disappear during

Table I. Average cycling efficiency (5-10 cycles) of lithium electrodes^a in PC, BL, and THF solutions. (The ratios between polarization of single galvanostatic processes of pure/contaminated systems are also indicated.) Currents are $0.5 \text{ mA}/\text{cm}^2$

System	Specification				
	No contamination	Oxygen saturated	Pure/O ₂	0.01M H ₂ O	Pure/H ₂ O
BL-LiClO ₄ 0.2-0.5M	<40%	80-85%	4 -	50%	2
BL-LiAsF ₆ 0.2-0.5M	60-65%	80-85%	3 -	—	—
PC-LiClO ₄ 0.2-0.5M	75-80%	85-90%	1.5-2	85-90%	2
PC-LiAsF ₆ 0.5M	80-85%	>90%	≈1	90%	1.25
THF-LiClO ₄ 0.2M	≈50%	60-65%	1.3	—	—
THF-LiClO ₄ 0.5M	75%	>85%	1.2	75%	0.9
THF-LiAsF ₆ 0.5M	95%	95%	1	<90%	0.8

^aLi electrodes were prepared by depositing lithium on nickel or copper substrates (several C/cm^2).

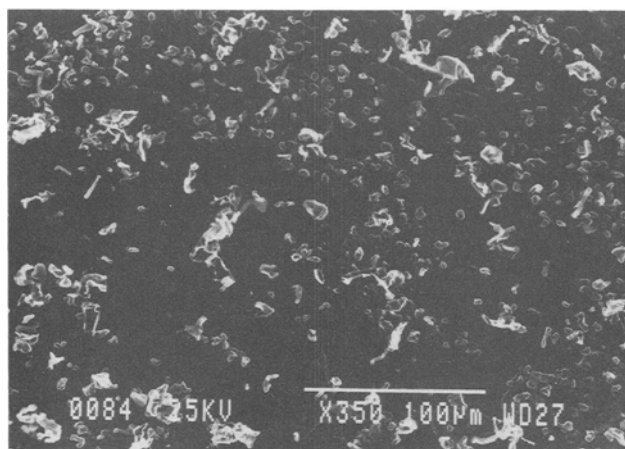
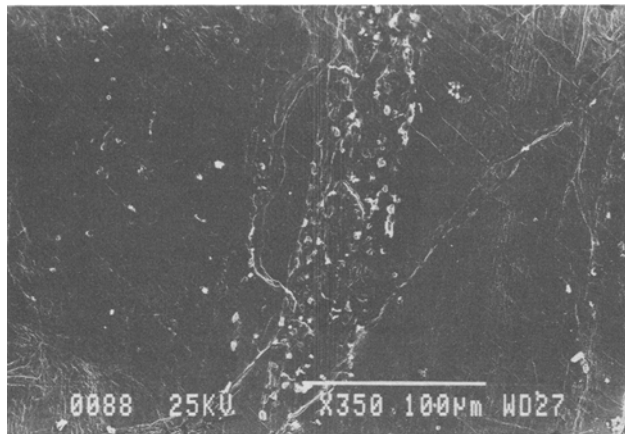


Fig. 7. SEM micrographs obtained from lithium surfaces on which lithium was deposited in THF/LiClO₄ 0.3M solutions (0.7 C/cm², 0.5 mA/cm²). Magnification = 350X. a) Oxygen saturated solution. b) Uncontaminated solution.

consecutive dissolution, as shown in Fig. 9c (obtained from lithium electrode on which lithium was deposited and consecutively dissolved in O₂-saturated LiClO₄-BL solution). Similar behavior was also observed with lithium electrodes cycled several times in O₂-saturated BL-LiClO₄ solutions followed by prolonged dissolution as the final step.

The reaction between lithium and oxygen may form several oxides, including Li₂O, Li₂O₂ (peroxide), and LiO₂[·] (superoxide). All of them are expected to be strong nucleophiles that can further react with the organic solvents. Indeed, in a previous work we found that lithium oxides nu-

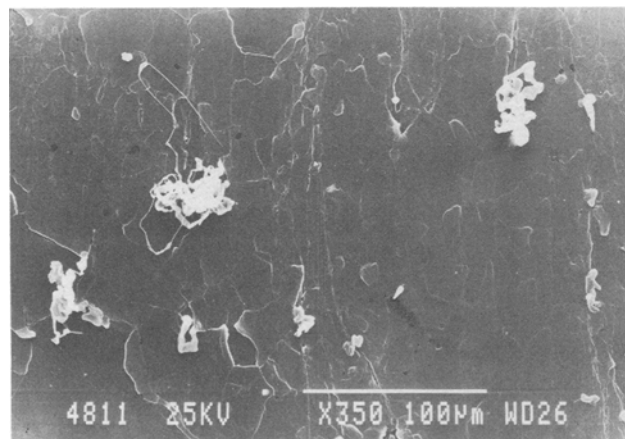


Fig. 8. Typical SEM micrograph of lithium surface on which lithium was deposited in oxygen-saturated PC-LiClO₄ 0.5M solution (0.6-0.7 C/cm², 0.5 mA/cm²). Magnification = 350X.

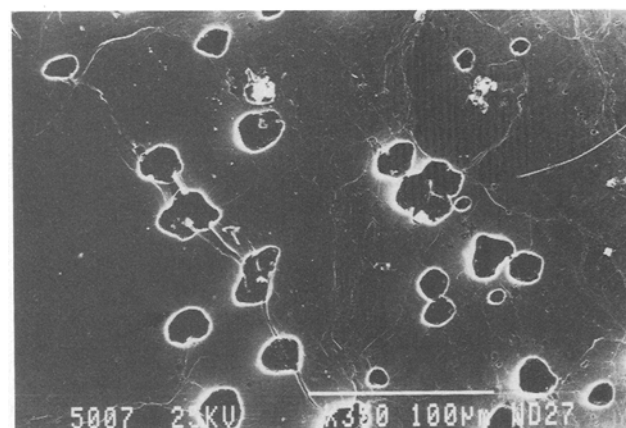
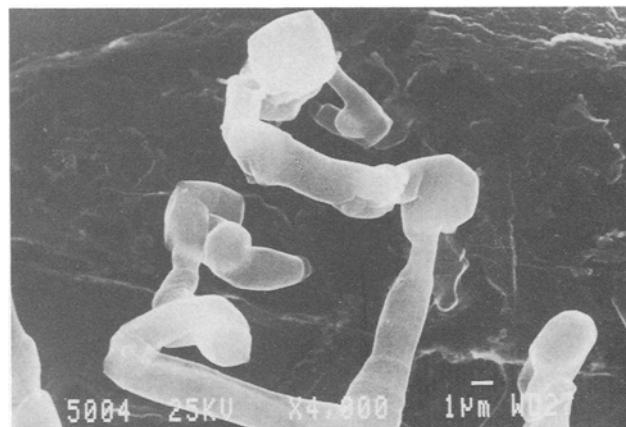
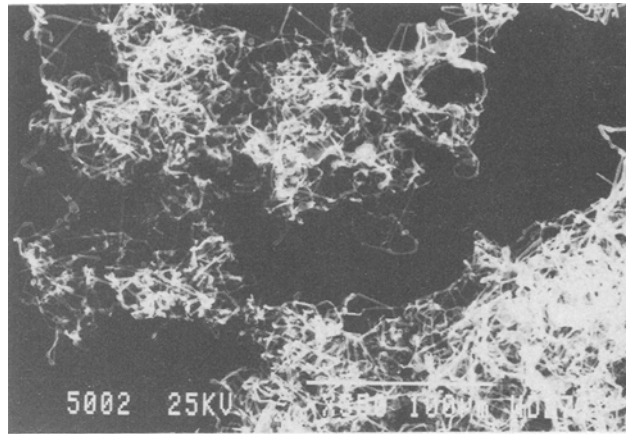


Fig. 9. SEM micrographs obtained from lithium electrodes on which lithium was deposited in oxygen saturated BL solutions (0.6-0.7 C/cm², 0.5 mA/cm²). a) Surface after lithium deposition, magnification = 350X, 0.5M LiClO₄ solution. b) A micrograph of a single dendrite, magnification = 4000X, 0.5M LiClO₄ solution. c) Same surface after consecutive dissolution (0.66-0.77 C/cm², 0.5 mA/cm²), 0.5M LiClO₄ solution, 350X.

cleophilically react with BL to form derivatives of γ -hydroxy butyric acid (11).

In the present work, it was found that PC is also nucleophilically attacked by oxides to form opened chain ROCO₂⁻ compounds (monoalkyl-carbonate anion). Figure 10 shows a FTIR spectrum obtained from superoxide (KO₂[·]) which was in contact with PC for 24h, followed by drying and pelletizing with KBr. This spectrum is typical of monoalkylcarbonate anion-alkaline metal salts. [ROCO₂⁻M⁺, M = Li, K, (12, 25), major peak assignments are also indicated in the figure.] Similar experiments with Li₂O also produced spectra which are typical of ROCO₂Li compounds. These compounds, having strong carbonyl absorptions in the IR around 1650 cm⁻¹ and 1350-1300 cm⁻¹, are also major components in surface films

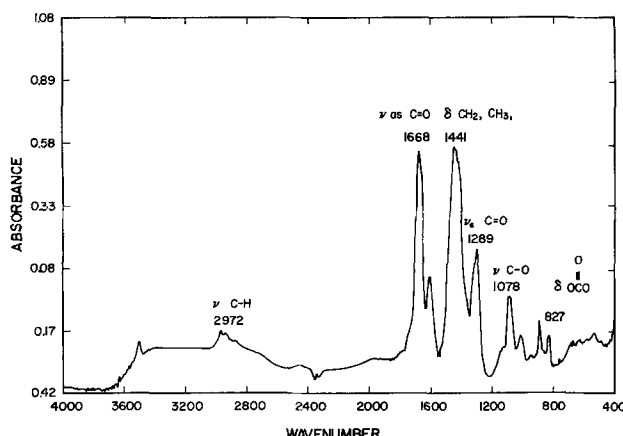


Fig. 10. FTIR spectrum obtained from KO_2^- , which was in contact for 24h with pure PC (KBr pellet). The spectrum is typical of ROCO_2K compounds (25). Main peak assignments appear in the figure.

formed on lithium in pure PC (12). These results show that PC reacts with oxides to form a bifunctional organic compound containing both OCO_2^- (carbonate anion) and C—O (alkoxy groups).

In this manner, PC resembles BL. THF, however, does not seem to react with lithium oxides. Since PC, BL, and ethers all react with lithium (11-13), and the saturation concentration of oxygen in these solvents is about $10^{-3}\text{-}10^{-4}\text{M}$ (26), it is questionable as to what degree oxygen dissolved in these solvents influences the surface chemistry of lithium in these systems.

We conducted a series of experiments in which identically pretreated lithium samples [pretreatment is described in Ref. (12)] were exposed for the same period of time to pure and oxygen-saturated solvents. The samples were all analyzed identically by surface-sensitive FTIR [protected with KBr plate, external reflectance mode (11, 12)].

Figure 11a shows a typical FTIR spectrum obtained from lithium surface exposed for two weeks to pure THF. The spectrum is typical of an alkoxide film [usually formed

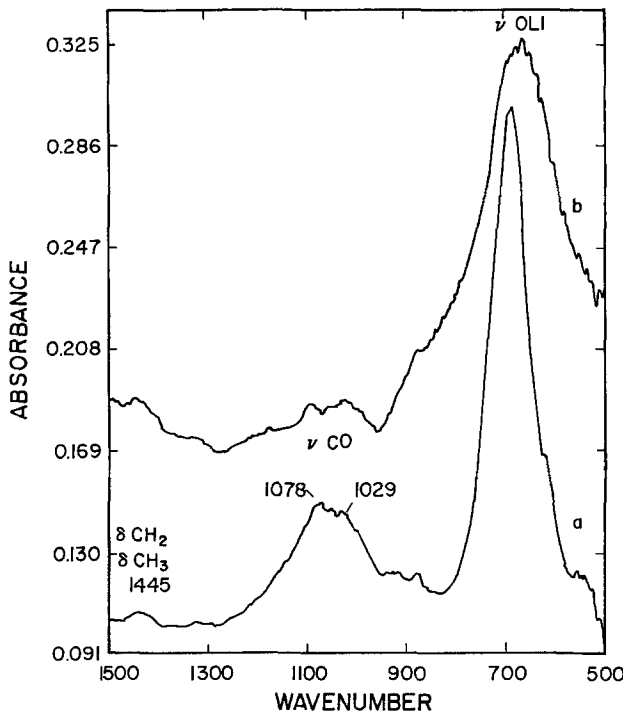


Fig. 11. Typical FTIR spectra obtained from lithium surfaces which were stored in THF for about 2 weeks. a) Pure THF. b) O_2 -saturated THF. The samples were identically treated and analyzed (same scale). Some peak assignments appear in the figure.

on lithium in ethereal solvents (13)]. Spectrum 11b was obtained from identically treated lithium surface which was exposed to O_2 -saturated THF. Spectrum 11b has a broad O-Li band around 650 cm^{-1} , which is broader than the similar O-Li band around 650 cm^{-1} shown in Fig. 11a. Also, the C-O peaks around 1100 cm^{-1} which are pronounced in Fig. 11a are absent or considerably diminished in spectrum 11b.

Figure 12 shows two typical FTIR spectra obtained from lithium surfaces treated in pure and O_2 -saturated PC [$6.6 \cdot 10^{-4}\text{M O}_2$ (26)]. Both spectra show the typical peaks of ROCO_2Li compounds, but the spectra obtained from lithium treated in O_2 -saturated PC have much more intense IR bands than the samples which were identically treated in pure PC.

Surface films formed on lithium in pure or oxygen-saturated BL both have pronounced carboxylate (CO_2^-) IR peaks around 1580 cm^{-1} and 1440 cm^{-1} . However, FTIR spectra obtained from lithium samples treated in O_2 -saturated BL have much stronger carboxylate peaks compared to samples treated identically in pure BL. In both cases, the reaction of the solvent with oxide films, if formed, produces species which are similar to those formed by direct reduction of the pure solvent by lithium. Therefore the presence of oxygen in solutions is not expected to change the main features in the IR spectra. However, the O_2 effect on the intensity of the absorption bands is significant.

All the above results point to the conclusion that O_2 modifies the surface chemistry of lithium in all the above solvents. In spite of the low saturation concentration [$10^{-3}\text{-}10^{-4}\text{M}$ (26)], dissolved oxygen seems to react with lithium faster than the solvents. Thus, an oxide layer is formed on the lithium surface. In the case of ethereal systems, the oxide film suppresses solvent reduction and no secondary film is formed. In cases of electrophilic solvents such as PC or BL, the primary oxide film reacts nucleophilically with the solvents to form a secondary film on top of the oxide layer.

Naturally, one would attribute the pronounced increase in intensity of IR bands of the surface films formed on lithium in the presence of oxygen to an increase in thickness. However, the lower overpotential required for electrochemical deposition and dissolution of lithium when O_2 is present as compared to uncontaminated solutions, seems to indicate that the oxygen-originated films are much thinner than those formed naturally by solvent reduction. Therefore, the 'intensity effect' mentioned above should be attributed to changes in the optical properties of the reflective metal-surface film systems, rather than to increase of thickness.

In the case of PC and THF, the oxygen-related films are probably more uniform than those formed in pure solvents, and therefore less dendrites are formed by lithium deposition in O_2 -contaminated systems. In the case of BL

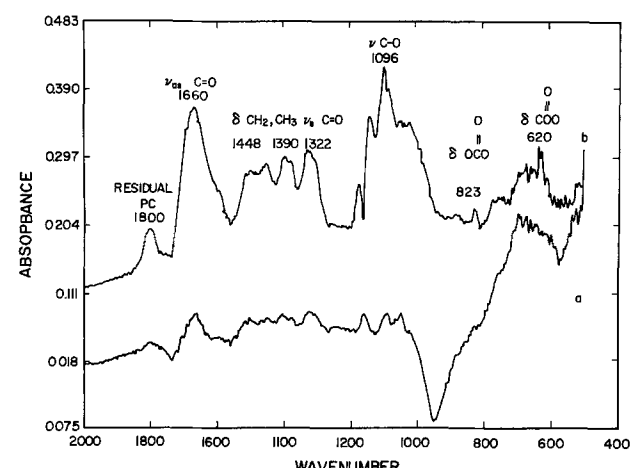


Fig. 12. Typical FTIR spectra obtained from lithium surfaces which were stored in PC for about 3 days. a) Pure PC. b) O_2 -saturated PC. The samples were identically treated and analyzed (same scale). Peak assignments appear in the figure [based on Ref. (12 and 25)].

Table II. The influence of traces of water on the IR spectra of components of surface films formed on lithium in the polar aprotic systems

Surface component	Systems formed	Most intense IR peaks of the dry compound, cm^{-1}	Additional IR peaks in compounds exposed to water traces, cm^{-1}
Li_2O	O_2 -contaminated	Around 600 broad ($\text{Li}-\text{O}$)	3675 (LiOH formation)
LiOH	H_2O -contaminated	3675 ($\text{H}-\text{O}$) 650-600 ($\text{Li}-\text{O}$)	3000, 1600, 1000, 850, 700
LiCl	LiClO_4 solutions	500-400	3500, 1700-1600
LiClO_4	—	1100-1050, 620	3500, 1600
ROLi	Ethers	2900-2700(CH), 1460-1440, 1370 ($\delta \text{CH}_2, \text{CH}_3$), 1100-1000 (CO)	3500, 1600
ROCO_2Li	PC	600-500 (LiO) 1650, ($\text{C}=\text{O}$), 1450 ($\delta \text{CH}_2, \text{CH}_3$), 1350-1290 ($\text{C}=\text{O}$), 1100-1050 ($\text{C}-\text{O}$), 820 (δOCO_2^-)	3675 (LiOH formation) 1520-1500, 1470-1450, 875 [Li_2CO_3 formation (12, 25)]
$\text{CH}_3\text{CH}_2\text{CH}_2\text{COOLi}$	BL	1590-1580, 1450-1440 (COO^-)	3500, 1600
Li_2CO_3	Wet PC	1520-1500, 1470-1450, 875	No change

the opposite may be true. However, when dendrites are formed in the O_2 -contaminated solutions they are protected quite efficiently from corrosion by the passivating oxide layers, and therefore in case of O_2 -contaminated BL solutions where massive dendrite formation occurs, these dendrites are not readily disconnected by corrosion of the bottlenecks but stay electrically connected to the bulk and, hence, are easily dissolved during discharge. Thereby, cycling efficiency of Li electrodes in this system increases compared to uncontaminated solutions.

The influence of water contamination.—We followed the hydration of several components of surface films formed on lithium in the solvent systems using FTIR. FTIR spectra of dry LiClO_4 , LiCl , $\text{CH}_3(\text{CH}_2)_2\text{COO-Li}$, CH_3OLi , $\text{CH}_3(\text{CH}_2)_3\text{OLi}$, $\text{CH}_3\text{OCO}_2\text{Li}$, $\text{CH}_3(\text{CH}_2)_2\text{OCO}_2\text{Li}$, Li_2CO_3 , Li_2O , and LiOH were measured (pelletized with KBr, or deposited on reflective gold or silver surfaces). Then, these compounds were exposed to humid air, followed by FTIR measurements. The results of these measurements are listed in Table II. It is clear that all of the above compounds are very sensitive to traces of water, and are easily hydrated, except for Li_2CO_3 . Li_2O , ROLi, and ROCO_2Li compounds also react with water to form LiOH or Li_2CO_3 as indicated in Table II.

Surface films formed on lithium in water-contaminated BL solutions ($>0.005\text{M}$) contain both LiOH and γ -hydroxy butyrate (11). Dissolved water reacts with lithium to form LiOH , which further nucleophilically attacks the solvent to form a secondary film of butyrate on top of the hydroxide. In this manner, the presence of water in BL leads to a modification of the surface films formed on lithium similar to the case of oxygen discussed above. Therefore, as shown in Table I, the presence of water in BL slightly improves the poor cycling efficiency of Li electrodes in the BL solutions and reduces the overpotential required for Li deposition and dissolution.

Surface films formed on lithium in THF-containing water concentration above 0.01M contains mostly LiOH (13). Part of the hydroxide film, close to the lithium side, is probably further reduced to Li_2O (27). At lower water concentration (0.005M and below), we could also detect the presence of alkoxides on lithium surfaces exposed to THF solutions. In ethers, water contamination seems to badly effect both surface morphology and cycling efficiency of the lithium electrodes. (See Table I; notice the increase in overpotential required for lithium dissolution or deposition when the ethereal solutions are contaminated with water.)

In the case of PC, the situation is different. LiOH , if formed, also reacts with PC to give ROCO_2Li species, which are somewhat similar to those formed on Li in pure PC (12). Water reacts with the ROCO_2Li compounds to give a stable Li_2CO_3 film (in addition to CO_2 and ROH). As shown in Table II, Li_2CO_3 is much less sensitive to water traces than any other compound formed on lithium surfaces in the polar aprotic systems. Therefore, trace water in PC solutions considerably increases cycling efficiency of lithium electrodes due to formation of Li_2CO_3 surface film, as shown in Table I. The decrease in polarization required

for lithium deposition and dissolution when PC solutions are contaminated with water is also indicative of significant modification of the surface films formed in this system resulting from the presence of water.

However, it is clear that water cannot serve as a reasonable surface film modification agent for lithium electrodes. Water, in contrast to oxygen and perhaps in contrast to any other active contaminant (e.g., CO_2 , N_2 , activated olefins), solvates most of the surface compounds that may be formed on lithium in polar aprotic systems. Consequently, there is no passivation against water in these systems. Thus, water contamination, which increases cycling efficiency in PC or BL solutions in short-term experiments, obviously completely reacts with lithium during prolonged storage. This situation is nicely demonstrated by morphology studies.

SEM studies of lithium electrodes treated in wet BL solutions (see Fig. 13) show the typical pronounced influence of water on lithium surface morphology. Lithium deposition forms dense dendrites on the surface. However, in contrast to pure or oxygen-contaminated solutions, where most of these dendrites disappear during consecutive dissolutions, those formed in the wet solution do not, and therefore the surface roughness increases from cycle to cycle. Apparently, most of these dendrites are electrically disconnected from the bulk. Similar results were obtained with Li electrodes treated in water-contaminated THF solutions. In the case of PC solutions, the effect of water on the Li surface morphology during short-term experiments is much less pronounced, probably because of the resistivity of the Li_2CO_3 film to water penetration.

The role of the salt anion.—Figure 14 shows SEM micrograph obtained from lithium surface on which lithium was deposited from O_2 -saturated LiAsF_6 -BL solution. Comparing this micrograph to those of Fig. 9 (obtained from Li surfaces treated in O_2 -saturated LiClO_4 -BL solution) demonstrates that lithium deposition in LiAsF_6 solutions is much smoother than in LiClO_4 . These electrolyte effects

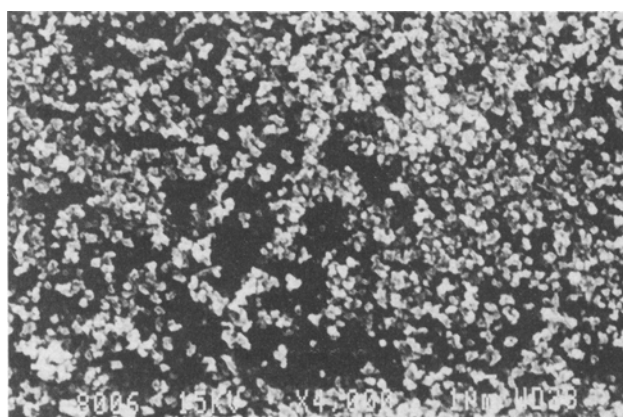


Fig. 13. Typical SEM micrograph of lithium surface treated in H_2O $0.01\text{M}/\text{LiClO}_4$ $0.5\text{M}/\text{BL}$ solution. Li was deposited on the Li surface ($0.6 \text{ C}/\text{cm}^2$, $0.5 \text{ mA}/\text{cm}^2$), followed by consecutive Li dissolution ($0.7 \text{ C}/\text{cm}^2$, $0.5 \text{ mA}/\text{cm}^2$). Scale = $0.25 \mu\text{m}/1 \text{ mm}$. Magnification = 4000X .

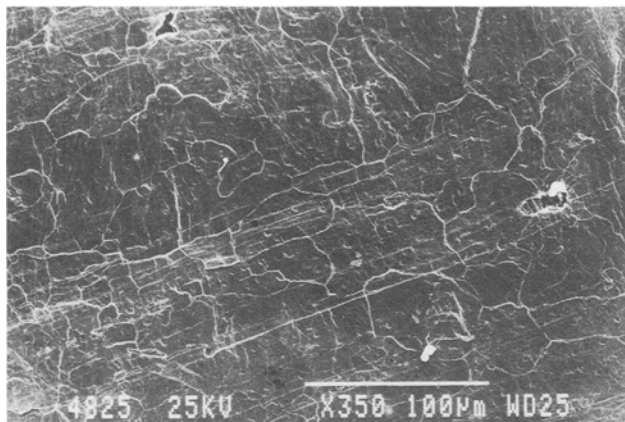


Fig. 14. A typical SEM micrograph of a Li surface on which lithium was deposited in LiAsF_6 0.5M/BL solution saturated with O_2 (0.6–0.7 C/cm^2 , 0.5 mA/cm^2). Magnification = 350X.

were observed with both pure and O_2 or H_2O -contaminated solutions of all three solvents. Hardly any dendrites are formed during lithium deposition in LiAsF_6 solutions. The morphology studies are consistent with the cycling efficiency measurements.

As shown in Table I, lithium electrodes in LiAsF_6 solutions have much higher cycling efficiency than in LiClO_4 solutions. Such a salt effect in ethers and PC was also observed by others (28). We studied salt reduction processes on Li electrodes in these solvents using XPS (12, 13), AES (29), SIMS (13), and x-ray microanalysis (23, 24). LiCl was always detected on Li surfaces treated with LiClO_4 solutions.

XPS measurements by us and others indicate that other chlorine compounds such as LiClO_3 may also be formed and precipitate on Li surfaces in LiClO_4 solutions (12, 13, 30). LiF is always detected on lithium electrodes in LiAsF_6 solutions. The FTIR measurements indicate that the nature of the salt does not change the surface chemistry of the organic films. Therefore, the pronounced salt effect on surface morphology and cycling efficiency of lithium electrodes may be related to the difference in the lithium halides, which precipitate on the lithium surfaces due to salt reduction.

In the case of LiClO_4 reduction, precipitation of more than a single type of chloride on the surface, and the size of the chloride anions, may distort homogeneous precipitation of the organic films. Thus, perhaps increasing the non-uniformity of the organic surface films increases the intensity of dendrite formation, and therefore influences cycling efficiency detrimentally. LiAsF_6 reduction precipitates only a single compound, LiF , on the surface. The fluoride anion is smaller than chloride, and therefore, LiF precipitation probably interferes far less with the uniformity of the organic surface films, compared to LiCl .

Conclusion

Li electrodes have low cycling efficiency in pure LiClO_4 solutions of PC, BL, and THF. [This correlates with surface morphology studies (SEM) which indicate dendritic deposition of lithium in these solutions.] The poor performance is understood in light of the complicated surface chemistry of lithium in these systems, which leads to a disordered precipitation of multi-functional organic surface species, together with insoluble lithium-chlorine salts.

Nevertheless, one should not give up the possibility of utilizing LiClO_4 solutions of PC or BL in secondary lithium batteries, since these systems are much less toxic, volatile, and resistant, compared to LiAsF_6 solutions of cyclic ethers (e.g., 1,3-dioxolane, 2-methyl THF) where much higher Li cycling efficiency is obtained. This work proves that surface modification of Li in the active solvents, by the use of chemicals which form better passive films, indeed considerably improves the performance of Li elec-

trodes in these systems. Thus, our results should encourage the use of active additives in electrolyte systems for secondary Li batteries as one of the preferred solutions for the problem of Li cycling efficiency in polar aprotic solvents.

Manuscript submitted July 22, 1988; revised manuscript received June 2, 1989.

REFERENCES

- K. M. Abraham and S. B. Brummer, in "Lithium Batteries," J. P. Gabano, Editor, Chapter 14, Academic Press, New York (1983).
- M. Garreau and S. Fouache Ayoub, in "Lithium Batteries," A. N. Dey, Editor, p. 240, The Electrochemical Society Softbound Proceedings Series, PV 87-1, Pennington, NJ (1987); C. Nanjundiah, J. L. Goldman, L. A. Dominey, and V. R. Koch, in "Primary and Secondary Ambient Temperature Lithium Batteries," J. P. Gabano, Z. Takehara, and P. Bro, Editors, p. 679, The Electrochemical Society Softbound Proceedings Series, PV 88-6, Pennington, NJ (1988).
- Y. Matsuda, *J. Power Sources*, **20**, 198 (1987).
- Y. Matsuda and M. Morita, *ibid.*, 273 (1987).
- E. Peled, *This Journal*, **126**, 2047 (1979).
- J. G. Thevenin and R. H. Muller, *ibid.*, **137**, 273 (1987).
- O. Bensenhard, J. Gurtler, P. Komenda, and A. Paxinos, *J. Power Sources*, **20**, 2153 (1987).
- S. B. Brummer, in "Lithium Nonaqueous Battery Electrochemistry," E. B. Yeager, B. Schumm, Jr., G. Blomgren, D. R. Blankenship, V. Leger, and J. Arkridge, Editors, p. 130, The Electrochemical Society Softbound Proceedings Series, PV 80-7, Pennington, NJ (1980).
- H. P. W. Lin and W. B. Ebner, in "The 32nd International Power Sources Symposium," p. 209, The Electrochemical Society, Pennington, NJ (1986).
- K. M. Abraham, *J. Power Sources*, **14**, 179 (1985).
- D. Aurbach, *This Journal*, **136**, 1606 (1989).
- D. Aurbach, M. L. Daroux, P. Faguy, and E. B. Yeager, *ibid.*, **134**, 1611 (1987).
- D. Aurbach, M. L. Daroux, P. Faguy, and E. B. Yeager, *ibid.*, **135**, 1863 (1988).
- D. Aurbach, M. L. Daroux, P. Faguy, and E. B. Yeager, Abstract 544, p. 772, The Electrochemical Society Extended Abstracts, Vol. 85-1, Toronto, Ontario, Canada, May 12-17, 1985.
- D. Aurbach, M. L. Daroux, P. Faguy, and E. B. Yeager, Submitted for publication.
- D. Aurbach, *This Journal*, **136**, 607 (1989).
- D. T. Sawyer, G. Chiericato, C. T. Angelis, E. J. Nanny, and T. Tsuchiya, *Anal. Chem.*, **54**, 1720 (1982).
- T. A. Lorenzola, B. A. Lopez, and M. C. Giordano, *This Journal*, **130**, 1359 (1983).
- D. Aurbach and H. Gottlieb, *Electrochim. Acta*, **34**, 141 (1989).
- S. I. Tobishima and A. Yamaji, *ibid.*, **28**, 1067 (1983).
- D. H. Shen, S. Subbarao, F. Deligiannis, and G. Halpern, Abstract 41, p. 57, The Electrochemical Society Extended Abstracts, Vol. 88-2, Chicago, IL, Oct. 9-14, 1988.
- K. M. Abraham, D. M. Pasquariello, and F. J. Martin, *This Journal*, **133**, 661 (1986).
- D. Aurbach, O. Yungman, and A. Meitav, *Electrochim. Acta*, To be published.
- D. Aurbach, O. Yungman, Y. Malik, and Y. Goffer, Unpublished results.
- V. W. Behrendt, G. Gatlow, and M. Drager, *Z. Anorg. Allg. Chem.*, **297**, 237 (1973).
- H. A. Frank and P. D. Lawson, in "Lithium Batteries," p. 354, The Electrochemical Society Softbound Proceedings Series, PV 81-4, Pennington, NJ (1981).
- D. Radman, Abstract 125, p. 188, The Electrochemical Society Extended Abstracts, Vol. 84-2, New Orleans, LA, Oct. 7-12, 1984.
- K. M. Abraham, J. L. Goldman, and D. L. Natwig, *This Journal*, **129**, 2404 (1982).
- D. Aurbach, G. Meckdugal, M. Daroux, and E. B. Yeager, Unpublished results.
- M. Froment, M. Garreau, J. Thevenin, and D. Warin, *J. Microscopie Spectr. Electron.*, **4**, 111, 483 (1979).